JOURNAL OF MATERIALS SCIENCE **38** (2003) 4471–4477

A combinatorial approach to surface anchored polymers

T. WU, M. TOMLINSON, K. EFIMENKO, J. GENZER
Department of Chemical Engineering, North Carolina State University, Raleigh, NC 27695-7905, USA
E-mail: jan_genzer@ncsu.edu

Recent advances in the field of self-assembly have led to the development of a plethora of new technologies derived from soft lithography that enable alternative ways of fabricating thin films with two- and three-dimensional patterns on material surfaces. Techniques involving the patterning of thicker polymer layers grafted to the substrate have been developed, based on selectively decorating the material surfaces with polymerization initiators and then performing the polymerization directly on the surface. Using this technology, the thickness of the overcoat film can be adjusted by simply varying the polymerization conditions (time, monomer concentration, polymerization temperature). Using these techniques, we have developed two simple methodologies that allow for combinatorial variation of selected properties of polymers anchored on surfaces, most notably the polymer grafting density and the polymer molecular weight.

1. Introduction

Recent advances in the field of self-assembly have led to the development of a plethora of new technologies derived from soft lithography [1] that enable alternative ways of fabricating two- and -three dimensional patterns on material surfaces. Many soft lithography techniques are based on controlled deposition of self-assembled monolayers (SAMs) [2]. Various structural patterns with dimensions ranging from hundreds of nanometers to several micrometers are created on the material surface using a "pattern-transfer element" or stamp that has a three-dimensional structure molded onto its surface. Because of the molecular nature of the SAMs, the surface patterns generated via soft lithography are thin—their thickness ranges typically from several Angstroms to several nanometers. Some applications, particularly those involving subsequent microfabrication steps, such as etching, require that thicker layers of the surface coating be formed. Hence, techniques involving the patterning of thicker polymer layers grafted to the substrate have been developed [3–10]. The latter group of technologies is based on selectively decorating the material surfaces with polymerization initiators and then performing the polymerization directly on the surface ("grafting from"). Using this technology, the thickness of the overcoat film can be adjusted by simply varying the polymerization conditions (time, monomer concentration, polymerization temperature).

While useful for creating substrates with well-defined dimensional chemical patterns of various shapes and dimensions, the soft lithography technologies always produce sharp boundaries between the distinct chemical regions on the substrate. However, for some applications, it is desirable that the physico-chemical characteristics, such as wetting of the substrate, change gradually. This can be accomplished by producing surfaces with a position-dependent and gradually varying chemistry. In these so-called "gradient surfaces," the gradient in surface energy is responsible for a position-bound variation in physical properties, most notably the wettability [11, 12]. Recent studies have reported on the preparation of molecular gradients on length scales ranging from nanometers to centimeters [13, 14, 30].

All gradient techniques presented to date led to the formation of two-dimensional gradient patterns. The manufacture of miniature devices and applications in lithography often requires the formation of three-dimensional structures. In this paper, we outline two simple methodologies that allow for combinatorial variation of selected properties of polymers anchored on surfaces, most notably the polymer grafting density and the polymer molecular weight (or equivalently length).

2. Anchored polymers with grafting density gradients

Surface anchored polymers with a grafting density gradient represent macromolecular systems, in which the number of polymers per unit area of the surface changes gradually as a function of the position on the surface. We will show that such structures can be prepared by first forming a concentration gradient of the polymerization initiator on the surface and followed by the "grafting from" polymerization [15, 24].

2.1. Formation and properties of the gradient initiator

We formed gradients of polymerization initiator on flat silica substrates using the methodology proposed

by Chaudhury and Whitesides [11]. Specifically, 1-trichlorosilyl-2-(*m*/*p*-chloromethylphenyl) ethane (CMPE) was mixed with paraffin oil (PO) and the mixture was placed in an open container that was positioned close to an edge of a silicon wafer. As CMPE evaporated, it diffused in the vapor phase and generated a concentration gradient along the silica substrate. Upon impinging on the substrate, the CMPE molecules reacted with the substrate ─OH functionalities and formed a SAM. The breadth and position of the CMPE molecular gradient can be tuned by adjusting the CMPE diffusion time and the flux of the CMPE molecules. The latter can be conveniently adjusted by varying the chlorosilane:PO ratio and the temperature of the CMPE:PO mixture. In order to minimize any physisorption of monomer and/or the polymer formed in solution on the parts of the substrate that do not contain the CMPE-SAM, we backfilled the unexposed regions on the substrate (containing unreacted ─OH functionalities) with *n*-octyl trichlorosilane, (OTS). After the OTS-SAM deposition, any physisorbed CMPE and OTS molecules were removed by thoroughly washing the substrates with warm deionized (DI) water (75°C, resistivity $> 16\ \mathrm{M\Omega \cdot m}$) for several minutes.

Fig. 1 shows the variation of the contact angle of deionized water, θ_{DIW}, on the CMPE-SAM covered substrate (closed circles) and the substrate that was backfilled with OTS-SAM (open circles) as a function of the position on the substrate. The CMPE source (CMPE:OTS ratio = 1:1) was allowed to diffuse for 2 min at 88°C, the OTS was deposited for 15 min at room temperature. The data in Fig. 1 illustrate that the contact angle of CMPE decreases gradually from ≈77° down to ≈0° as one moves across the substrate starting at the CMPE side. The open circles indicate that after the OTS deposition, the regions on the substrate far from the diffusing source are covered with a complete OTS monolayer ($\theta_{\mathrm{DIW}} \approx 100°$). As one traverses across the CMPE gradient, the contact angle decreases from ≈100° (OTS side) down to ≈88° (CMPE side). The minute increase of the contact angle within the CMPE-SAM is likely a result of a small interpenetration of OTS into the CMPE SAM.

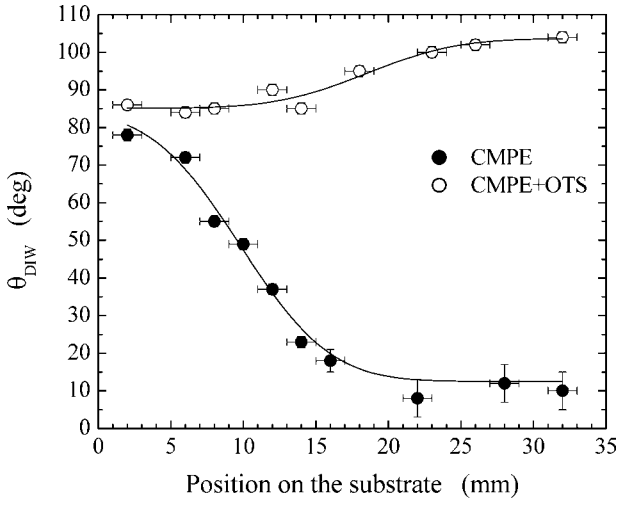

Figure 1 Dependence of the DI water contact angle, θ_{DIW}, on the position along the gradient substrate measured after the CMPE-SAM formation (solid circles) and after backfilling with the OTS-SAM (open circles) (From [24]).

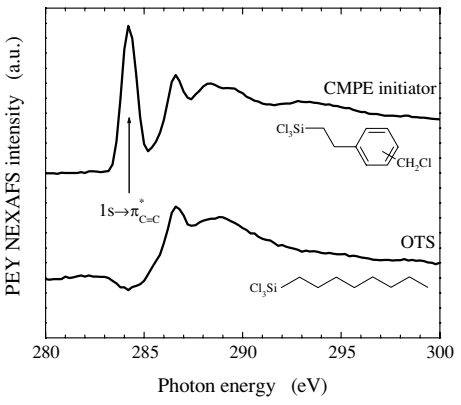

Figure 2 Carbon K-edge PEY NEXAFS spectra collected from the CMPE (top) and OTS (bottom) SAMs. The arrow marks the position of the $1s \rightarrow \pi^*$ transition for phenyl C═C, present only in the CMEP-SAM specimen (From [24]).

Near-edge X-ray absorption fine structure (NEXAFS) spectroscopy was used to provide detailed chemical and structural information about the SAMs on the substrate [16, 17]. The NEXAFS spectra were collected in the partial electron yield (PEY) at the normal ($\theta = 90°$), grazing ($\theta = 20°$), and so-called "magic" angle ($\theta = 55°$) incidence geometries, where θ is the angle between the sample normal and the polarization vector of the X-ray beam. In Fig. 2 we plot the carbon edge K-edge PEY NEXAFS spectra taken from the CMPE-SAM (top) and OTS-SAM (bottom) samples. The NEXAFS spectra collected at the "magic" angle were indistinguishable from those recorded at the normal and grazing incidence geometries, revealing that the CMPE-SAMs are not oriented, rather they formed a "liquid-like" structure. This observation is in accord with recent studies from Chaudhury and Allara groups who studied the transition between the "liquid-like" and "semi-crystalline-like" structures in hydrocarbon SAMs [18]. The NEXAFS spectra in Fig. 2 both contain peaks at 286.0 and 288.5 eV that correspond to the $1s \rightarrow \sigma^*$ transition for the C─H and C─C bonds, respectively. In addition, the spectrum of CMPE also exhibits a very strong signal at 284.2 eV, which can be attributed to the $1s \rightarrow \pi^*$ transition for phenyl C═C (cf. Fig. 2) [16]. The latter signal can thus be used as an unambiguous signature of CMPE in the sample. With the X-ray monochromator set to 284.2 eV, we collected the PEY NEXAFS signal by rastering the X-ray beam across the gradient. The lines in Fig. 3 show the variation of the PEY NEXAFS intensity measured at 284.2 eV across the gradient samples prepared by diffusing CMPE for 2 min from mixtures with various CMPE:PO ratios equal to 1:1 (solid line), 1:2 (dashed line), 1:5 (dotted line), and 1:10 (dash-dotted line). In the reminder of the paper, we refer to such substrates as S1, S2, S5, and S10, respectively. The data in Fig. 3 reveal that the PEY NEXAFS intensity from the C═C phenyl bond, and thus the concentration of CMPE in the sample, decreases as one moves from the CMPE side of the sample towards the OTS-SAM; the functional form closely resembles that of a diffusion-like profile. Experiments using variable angle spectroscopic ellipsometry

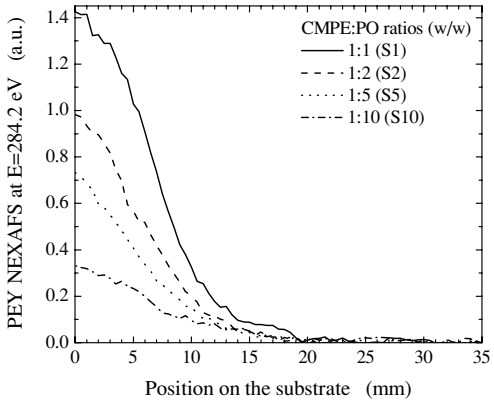

Figure 3 PEY NEXAFS intensity at $E = 284.2$ eV as a function of the position the substrates containing the initiator gradients made from mixtures of various CMPE:OTS ratios (w/w) equal to 1:1 (solid line), 1:2 (dashed line), 1:5 (dotted line), and 1:10 (dash-dotted line) (From [24]).

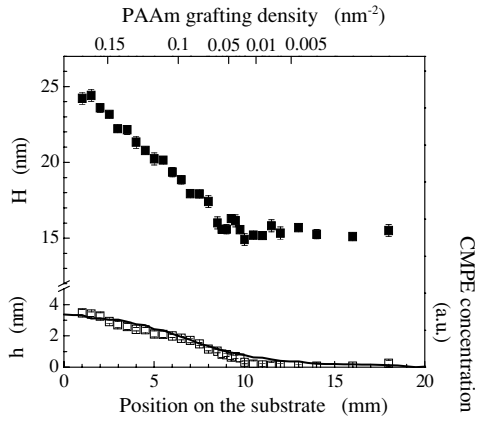

Figure 4 Dry (h, open squares) and wet (H, closed squares) thickness of the PAAm brush and the CMPE concentration (solid line) as a function of the position on the substrate S1 (CMPE:PO concentration = 1:1) (From [15]).

(VASE) confirmed that only a single monolayer was formed along the substrate.

2.2. "Grafting from" on the gradient initiator surfaces

The polymerization of poly(acryl amide) (PAAm) was performed by atom transfer radial polymerization (ATRP), as described earlier [19–21]. After the reaction, any physisorbed monomeric and polymeric acrylamide was removed by soxhlet extraction with deionized water for 48 h and dried with nitrogen. In addition, PAAm brushes were grown on silica gels (Davisil^{TM}, grade 645, surface area ≈300 m^2/g) using the procedure outlined in [20]. The PAAm polymers were grown and purified using the same conditions as described above. The PAAm chains were then cleaved from the silica support with a 10% (w/w) solution of HF for 2 h, neutralized by adding sodium carbonate and filtered. Size exclusion chromatography was used to analyze the molecular weight of the cleaved PAAm macromolecules ($M_w = 17$ kDa, polydispersity index = 1.7) [24]. We note that Huang and Wirth reported a value of $M_w = 15.6$ kDa for the concentration of monomer, polymerization temperature and time that were the same as in our experiments [20].

2.3. Properties of grafted polymer layers

VASE was used to measure the thickness of the dry polymer film, h, as a function of the position on the substrate. The results for the PAAm gradient prepared on the S1 substrate are shown in Fig. 4. The data in Fig. 4 reveal that h decreases gradually as one moves across the substrate starting at the CMPE edge. Note that the concentration profile of the polymer follows that of the CMPE initiator (solid line in Fig. 4). Because the polymers grafted on the substrate have all roughly the same number of segments (see discussion below), the variation of the polymer film thickness can be attributed to the difference in the density, σ, of the CMPE grafting points on the substrate. The grafting density can be calculated from $\sigma = h\rho N_A/M_w$, where ρ is the density of PAAm (=1.302 g/cm^3), N_A is the Avogadro's number, and M_w is the polymer molecular weight.

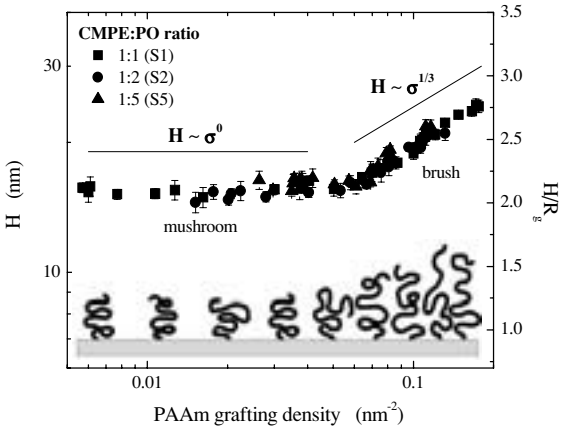

Figure 5 Wet thickness of the PAAm brush (H) as a function of the PAAm brush grafting density (σ). The schematic illustrates the conformations of the surface-anchored PAAm as a function of the grafting density (From [24]).

The substrates with the grafted PAAm were placed into a solution cell that was filled with DI water (pH ≈ 7), a good solvent for PAAm, and incubated for at least 5 h. The wet thickness of grafted PAAm in DI water, H, was measured using VASE. The values of H for samples prepared on CMPE:PO = 1:1 gradients are shown in Fig. 4. The data show that H decreases as one traverses across the substrate stating at the CMPE side. Similar experiments were performed with PAAm brushes grown from gradient CMPE substrates prepared from various CMPE:PO concentrations.

In Fig. 5 we plot the wet polymer thickness as a function of the PAAm grafting density on the substrate. The data in Fig. 5 reveal that at low σ, H is independent of the grafting density. Hence the chains are in the mushroom regime. At higher polymer grafting densities, H increases with increasing σ, indicating the brush behavior. The crossover between the two regimes occurs at $\sigma \approx 0.065$ nm^{-2}. By fitting the data in the brush regime to $H \sim N\,\sigma^n$ we obtain n equal to 0.37 ± 0.04 (substrate S1), 0.39 ± 0.05 (substrate S2), and 0.40 ± 0.06 (substrate S5). We note that n obtained by fitting the experimental data is slightly higher that the predicted value of $n = 1/3$; this observation is in agreement with recent reports [22]. A remark has to be made about

the possible variation of the chain length with grafting density. Jones and coworkers recently reported on studies of grafting from polymerization of poly(methyl methacrylate) using ATRP from substrates having various surface densities of the polymerization initiator, ω-mercaptoundecyl bromoisobutyrate [23]. Their study revealed that the grafting density of the polymer depends on the grafting density of the initiator. However, based on the data presented in [23] it is uneasy to discern whether the kinetics of the polymerization also depends on the grafting density of the initiator. Currently we have no means of measuring the molecular weight of the grafted brushes directly on the gradient substrate. While we cannot exclude the possibility that the length PAAm chains polymerized on the various parts of the molecular gradient substrate varies with σ, we note that the fact that the curves in Fig. 5 superimpose on a single master curve indicates that the polymers have likely very similar lengths, which is not surprising for the rather short anchored polymers synthesized in this work.

In addition to the measurement of the wet brush thickness, we have also performed wettability experiments as a function of the PAAm grafting density on the substrate [24]. Our aim was to corroborate the ellipsometric data and provide more insight into the polymer packing in the surface grafting density gradient. In Fig. 6 we plot the dry PAAm thickness, h, (closed symbols) and the contact angles of DI water, θ_{DIW}, (open symbols) as a function of the position on the substrate for samples prepared on the S1 (squares) and S5 (triangles) substrates. In both samples, the dry thickness of PAAm decreases gradually as one moves across the substrate starting at the CMPE edge. The θ_{DIW} values increase as one traverses across the substrate stating at the CMPE side. The increase in θ_{DIW} is not monotonous, it follows a "double S"-type shape. While the "double S"-type dependence of θ_{DIW} on the position on the sample is detected in both S1 and S5 samples, there are differences in the plateau values. Specifically, while for the S1 sample, the three plateaus are located at $\theta_{\mathrm{DIW}} \approx 40^\circ$, $\approx 83^\circ$, and $\approx 100^\circ$ the corresponding values for the S2 sample are $\theta_{\mathrm{DIW}} \approx 47^\circ$, $\approx 70^\circ$, and $\approx 97^\circ$. Based on the dry thickness data and our previous discussion, the three plateaus in the contact angle behavior can be attributed to the wetting characteristics inside the brush, mushroom, and OTS (no PAAm) regions. At distances far away from the CMPE edge, where the θ_{DIW} values are high, there is no grafted PAAm on the sample. The contact angle experiments detect the presence of the OTS monolayer. By moving closer towards the CMPE edge, the contact angles decrease by $\approx 20-30^\circ$ indicating that some polymers are present on the substrate. However, their grafting densities are low so that the probing liquid can penetrate between the grafted chains; the measured contact angles represent a weighted average between the PAAm and OTS. Upon approaching the mushroom-to-brush transition region, the contact angle further decreases. The decrease is steeper for PAAm on the S1 substrate and more gradual for the S2 sample, indicating that the density of PAAm increases more rapidly in the former case. The contact angles in the lowest plateau are $\theta_{\mathrm{DIW}} \approx 40^\circ$ and $\approx 47^\circ$ for samples S1 and S5, respectively. In independent experiments, we have established that the θ_{DIW} of a pure PAAm is ≈ 35–38° [25]. Because in both cases the PAAm polymers grafted on the substrate have roughly the same degree of polymerization, the variation of the polymer film thickness can be attributed to the difference in the density of the CMPE grafting points on the substrate. Specifically, close to the CMPE edge, the PAAm macromolecules form a dense brush on the S1 substrate and a "semi-dense" brush on the S5 substrate.

The previous discussion revealed that θ_{DIW} depends on the grafting density of the PAAm chains on the substrate. Earlier we have shown that the wet thickness of PAAm prepared on substrates with various CMPE concentrations can be collapsed on a single master curve when plotted as H vs. σ. One would thus expect that also the wettabilities of the substrates plotted versus the PAAm grafting density should exhibit similar universal behavior. In Fig. 7 we plot the negative cosine of θ_{DIW} as a function of the grafting density of PAAm on substrates S1 (squares) and S5 (triangles). As anticipated, the data collapse on a single master curve. A close inspection of the results present in Fig. 7 shows that the data can be divided into three distinct regions. For

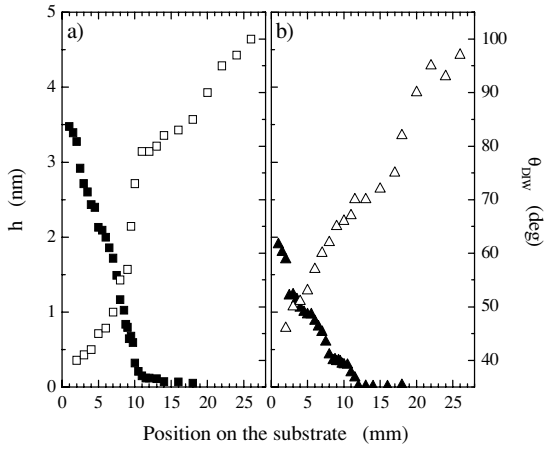

Figure 6 Dry thickness of PAAm (h, closed symbols) and contact angle of DI water (θ_{DIW}, open symbols) as a function of the position on the substrate for samples prepared on the S1 and S5 substrates (From [24]).

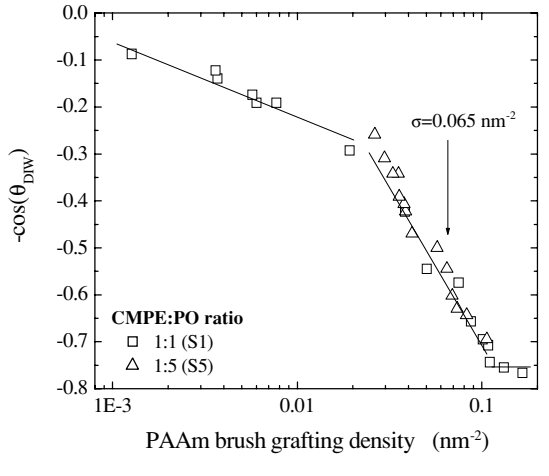

Figure 7 Negative cosine of the contact angle of DI water as a function of the PAAm grafting density on the substrate for samples prepared on the S1 and S5 substrates. The lines are meant to guide the eyes (From [24]).

$\sigma > 0.1\ \mathrm{nm}^{-2}$, the chains are expected to be in a brush regime—the wettabilities are close to the pure PAAm ($-\cos(\theta_{\mathrm{DIW}}) \approx -0.79$). For $\sigma < 0.011\ \mathrm{nm}^{-2}$ the PAAm chains form mushroom conformations on the substrate. In this regime, the wettabilities change slightly because the distance between the chains also changes, although they are already loosely separated on the substrate. At grafting densities $0.011\ \mathrm{nm}^{-2} < \sigma < 0.1\ \mathrm{nm}^{-2}$, the slope of $-\cos(\theta_{\mathrm{DIW}})$ changes rather rapidly. The data in Fig. 7 show that the position of the mushroom-to-brush crossover determined using the wettability approach is in accord with the ellipsometric measurements (the transition location was established to be at $\sigma \approx 0.065\ \mathrm{nm}^{-2}$). However, in the former case, the transition region extends over almost one order of magnitude in σ, which is broader, as expected [26–28], that the transition region predicted by the H vs. σ data. We speculate that the small difference between the widths of the mushroom-to-brush region inferred from both types of experiments is likely associated with the inaccuracy in H, which was obtained indirectly by the model fitting of the VASE data.

3. Anchored polymers with molecular weight gradients

In addition to the polymer grafting density, polymer molecular weight is another important molecular parameter that influences profoundly the properties of surface-anchored polymers. The thickness of the anchored polymer layers is proportional to the degree of polymerization of the anchored polymer. For some applications, it would be convenient to have samples with anchored polymers having variable degrees of polymerization.

3.1. Polymer brushes with gradients in length

We have recently designed a method leading to the preparation of surface-anchored polymers with a variable degree of polymerization [31]. The samples are prepared in a polymerization chamber with a vertically positioned sample holder. Tubing, attached at the bottom of the chamber, is connected to a micropump, which controls the flow rate removal of the solution from the chamber. The brush formation proceeds as follows. The chamber is initially loaded with a solution comprising a monomer, bipyridine, $CuCl_2$, and the solvent. The chamber is purged with nitrogen for a couple of minutes in order to remove any oxygen present. CuCl is added and the silicon wafer, covered with a chemisorbed initiator, is lowered into the solution. The polymerization proceeds following the standard scheme [29]. During the reaction, the micropump removes the solution from the chamber causing a steady decrease in the vertical position of the 3-phase (substrate/solution/inert) contact line. The profile (including the "steepness") of the polymer brush length gradient on the substrate is controlled by varying the removal rate of the polymerization solution.

Poly(methyl methacrylate) with a variable degree of polymerization anchored to silica surfaces was synthesized following the room-temperature ATRP polymerization scheme described earlier [8]. In the main part of Fig. 8 we plot the variation of the PMMA brush thickness after drying (measured by ellipsometry) as a function of the position on the substrate. The inset depicts the variation of the same quantity but as a function of the polymerization time. The data in the inset illustrate that, as expected, the thickness increases linearly with polymerization time, in accord with previous reports [8, 29]. We have tested the feasibility of varying the solution removal speed. The arrows in Fig. 8 mark the instances where the exhaust speed was reduced two times during the polymerization. As apparent from the data, the polymerization rate as a function of time was not affected (inset) but the "steepness" of the gradient increased correspondingly.

Our experiments revealed that the parameters of the polymer brush—notably the polymer growth rate and polydispersity—are controlled by the amount of $CuCl_2$ added to the reaction vessel (cf. Fig. 9) [31]. This finding is not that surprising given the nature of the

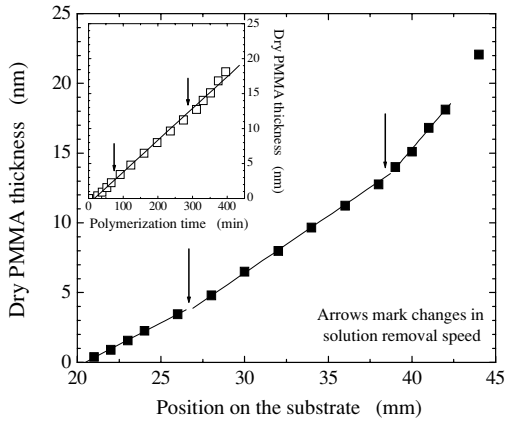

Figure 8 Thickness of PMMA as a function of the position on the substrate. The inset shows the dependence of the PMMA brush length as a function of the polymerization time. The ATRP polymerization was performed at room temperature by mixing methyl methacrylate monomer (32.7 g), methanol (25.5 g), DI water (7.0 g), bipyridine (2.06 g), CuCl (0.66 g), and $CuCl_2$: (0.04 g). The arrows mark changes in the solution removal speed (From [31]).

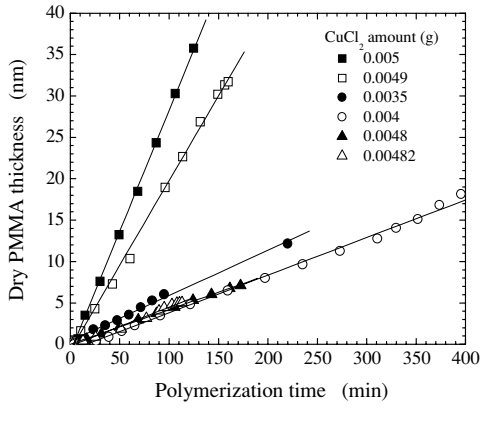

Figure 9 Dry PMMA brush thickness as a function of the room temperature polymerization time and various concentrations of $CuCl_2$. The amounts of other reagents are: methyl methacrylate monomer (32.7 g), methanol (25.5 g), DI water (7.0 g), bipyridine (2.06 g), and CuCl (0.66 g). The lines are meant to guide the eyes.

reaction. The key reaction in ATRP is the reversible activation-deactivation process using metal (M)/ligand (L) complexes:

$$P - X + M^{\mathrm{I}}X/2L \underset{\rightarrow}{\longleftarrow} P^* + M^{\mathrm{II}}X_2/2L,$$

where M is usually Cu, X is Cl or Br. The propagating radical, P^*, produced by the halogen atom transfer from $P - X$ to the $M^{\mathrm{I}}X/2L$ complex will undergo polymerization until it is deactivated by the $M^{\mathrm{II}}X_2/2L$ complex. The quick speed of the activation-deactivation cycles compared to rate of polymerization and the low concentration of the active species (relative to the $P - X$ ones) lead to polymers with narrow polydispersities. MCl_2 is usually added to the reaction mixture to regulate the reaction rate and chain polydispersity. We believe that the combinatorial design of our system is conveniently suited for such studies because it allows for complete probing of the anchored polymer properties and studying the polymerization kinetics in confined geometries [31].

3.2. Polymer brushes with gradients in chemistries

A nice feature of the set up is the ability to create complex architectures that would otherwise be difficult to build. For example, the brush length gradient of poly(methyl methacrylate) (PMMA), can be subsequently immersed into a solution of another monomer, say styrene, thus forming a grafted diblock copolymer PS-b-PMMA. This set up is possible because the PMMA brush acts as a living macroinitiator for the subsequent polymerization of PS. Depending on which side of the styrene length gradient is immersed first into the styrene solution, either a copolymer brush with a variable length but a constant composition (longer PMMA chains first), or a copolymer with a constant length but variable composition (shorter PMMA chains first) is formed. In the previous example, we assumed for simplicity that the rates of immersion will be adjusted such that the rates of polymerization of styrene and methacrylate would be equal.

We have succeeded in preparing the first polymer composition gradient brush anchored on the solid substrate [32]. Specifically, we have first anchored poly(hydroxylethyl methacrylate) (PHEMA) brush with a molecular weight gradient. The sample was then rotated vertically and immersed in the solution containing MMA, bipyridine and $CuCl/CuCl_2$ in a water/methanol solution. The PHEMA sample acted as a macroinitiator, hence a PHEMA-b-PMMA copolymer was produced. The data Fig. 10 show the dry thickness measured by ellipsometry on the PHEMA brush (closed squares), PMMA brush in PHEMA-b-PMMA (open squares), and the total PHEMA-b-PMMA brush (crosses squares) as a function of the position on the substrate. The idea behind this experiment was to prepare a copolymer with a gradual variation of the composition and a constant total thickness. The data in Fig. 10 show that we have succeeded only partially. While there is a clear variation of the composition along

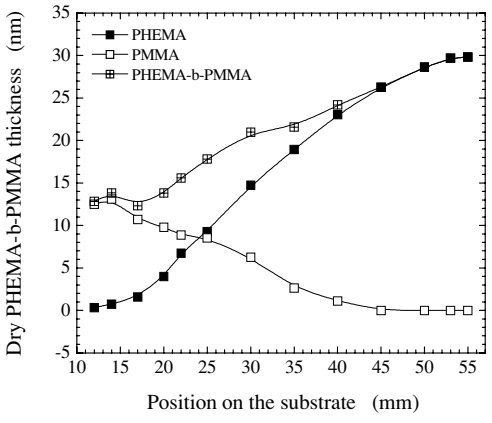

Figure 10 Dry thickness of PHEMA block (closed squares), PMMA block (open squares), and the total PHEMA-b-PMMA thickness (crossed squares) as a function of the position on the substrate. The upper part of the figure shows the DI water contact angles measured on the PHEMA-b-PMMA brush.

the copolymer, the total thickness of the PHEMA-b-PMMA copolymer does not stay constant. Several parameters are expected to influence the properties of the copolymers. First, the activity of the macroinitiator (PHEMA in this case) would crucially depend on the length. Second, we may be suffering from complications in wetting at the three-phase contact line meniscus. Considering that the initiator-covered substrates are hydrophobic and that the PHEMA grown onto the substrate is slightly hydrophilic, the meniscus shape and the wetting angle may initially change during the polymerization. This may explain the concave thickness profile of PHEMA in the initial stages of the polymerization. While more work is needed to fine-tune the preparation of polymers with a variable molecular weight anchored on substrates, the results discussed here illustrate the feasibility of the novel strategy for preparing combinatorial polymer brushes with a variable molecular weight and chemical composition.

4. Summary

We have presented two new fabrication methods leading to the formation of combinatorial surface-grafted polymers. We have shown that polymer brushes with gradient variation of their grafting densities on solid substrates can be generated by first depositing molecular gradients of polymerization initiators on solid silica-covered substrates, and performing polymerization from the substrate bound initiator centers ("grafting from"). We have also outlined a method for preparing assemblies comprising arrays of polymer brushes with a variable polymer molecular weight. We have shown that the latter methodology can be extended to prepare complex combinatorial brush structures with variable chemistries and morphologies.

Acknowledgement

This research was supported by the National Science Foundation, Grant No. CTS 0209403, The Camille Dreyfus Teacher-Scholar award, and The 3M Non-Tenured Faculty award. The NEXAFS experiments

were carried out at the National Synchrotron Light Source, Brookhaven National Laboratory, which is supported by the U.S. Department of Energy, Division of Materials Sciences and Division of Chemical Sciences. We thank Drs. Petr Vlček, Vladimír Šubr (both Institute of Macromolecular Chemistry, Prague), and Daniel A. Fischer (NIST) for their collaboration.

References

1. Y. XIA and G. M. WHITESIDES, *Angew. Chem. Int. Ed. Engl.* **37** (1998) 550; Y. XIA, *et al.*, *Chem. Rev.* **99** (1999) 1823.
2. A. ULMAN, "An Introduction to Ultrathin Organic Films from Langmuir-Blodgett to Self Assembly" (Academic Press, New York, 1991).
3. M. HUSSEMAN, *et al.*, *Angew. Chem. Int. Ed. Engl.* **38** (1999) 647.
4. R. SHAH, *et al.*, *Macromolecules* **33** (2000) 597.
5. N. L. JEON, *Appl. Phys. Lett.* **75** (1999) 4201; N. KIM, *et al.*, *Macromolecules* **33** (2000) 3793.
6. B. DE BOER, *et al.*, *ibid.* **33** (2000) 349.
7. P. GHOSH, *et al.*, *ibid.* **34** (2001) 1230.
8. D. M. JONES and W. T. S. HUCK, *Adv. Mater.* **13** (2001) 1256.
9. J. HYUN and A. CHILKOTI, *Macromolecules* **34** (2001) 5644.
10. V. L. OSBORNE, D. M. JONES and W. T. S. HUCK, *Chem. Comm.* (2002) 1838.
11. M. K. CHAUDHURY and G. M. WHITESIDES, *Science* **256** (1992) 1539.
12. J. GENZER, "Molecular Gradients: Formation and Applications in Soft Condensed Matter Science," Encyclopedia of Materials Science, edited by K. H. J. Buschow, R. W. Cahn, M. C. Flemings, B. Ilschner, E. J. Kramer and S. Mahajan, (Elsevier, Oxford, in press, 2002).
13. K. EFIMENKO and J. GENZER, *Adv. Mater.* **13** (2001) 1560.
14. R. R. FUIERER, *et al.*, *ibid.* **14** (2002) 154.
15. T. WU, K. EFIMENKO and J. GENZER, *J. Amer. Chem. Soc.* **124** (2002) 9394.
16. J. STÖHR, "NEXAFS Spectroscopy" (Springer-Verlag, Berlin, 1992).
17. The NEXAFS Experiments were Carried Out on the U7A NIST/Dow Materials Soft X-ray Materials Characterization Facility at the National Synchrotron Light Source at Brookhaven National Laboratory (NSLS BNL).
18. M. K. CHAUDHURY and M. J. OWEN, *J. Phys. Chem.* **97** (1993) 5722; D. L. ALLARA, A. N. PARIKH and E. JUDGE, *J. Chem. Phys.* **100** (1994) 1761.
19. X. HUANG, L. J. DONESKI and M. J. WIRTH, *Chemtech* **19** (Dec 1998); *Idem.*, *Anal. Chem.* **70** (1998) 4023.
20. X. HUANG and M. J. WIRTH, *Macromolecules* **32** (1999) 1694.
21. T. WU, K. EFIMENKO and J. GENZER, *ibid.* **34** (2001) 684.
22. S. WAMAMOTO, *et al.*, *ibid.* **33** (2000) 5608.
23. D. M. JONES, A. A. BROWN and W. T. S. HUCK, *Langmuir* **18** (2002) 1265.
24. T. WU, K. EFIMENKO, P. VLČEK, V. ŠUBR and J. GENZER, *Macromolecules* **36** (2003) 2448.
25. In Order to Measure the Contact Angle of DI Water on Pure PAAm, We Have First Grown PAAm From a Substrate Covered Homogeneously with the CMPE Initiator. The Polymerization Conditions were the Same as for the Sample Described in the Text. The Contact Angle was Determined Using the Technique Described in the Text.
26. M. S. KENT, *Macromol. Rapid Commun.* **21** (2000) 243 and References Therein.
27. J. F. DOUGLAS, *et al.*, "Polymer Brushes: Structure and Dynamics," Encyclopedia of Materials: Science and Technology (Elsevier, 2001) p. 7218.
28. M. A. CARIGNANO and I. SZLEIFER, *Macromolecules* **28** (1995) 3197; I. SZLEIFER, *Curr. Opin. Colloid Interface Sci.* **1** (1996) 416; I. SZLEIFER and M. A. CARIGNANO, *Adv. Chem. Phys.* **XCIV** (1996) 165.
29. T. E. PATTEN and K. MATYJASZEWSKI, *Adv. Mater.* **10** (1998) 901 and References Therein.
30. S.-H. CHOI and B. ZHANG NEWBY, *Langmuir* **19** (2003) 7427.
31. M. R. TOMLINSON and J. GENZER, *Macromolecules* **36** (2003) 3449.
32. *Idem.*, *Chem. Comm.* No. 12 (2003) 1350.